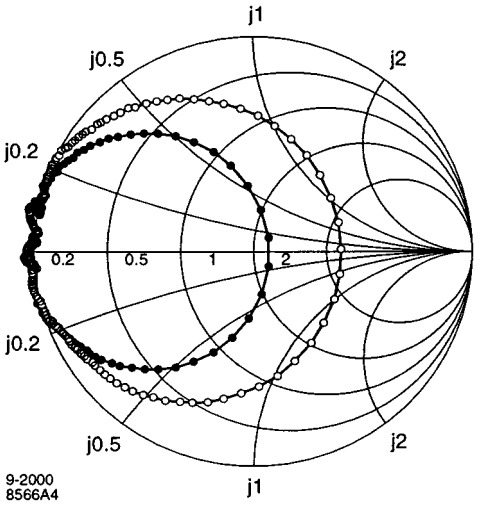

Fig. 4. Smith Chart plot of measured S_{11} for the case of no beam port (black) and with a 680-μm beam port (white). For both cases, we see that the cavity is overcoupled.

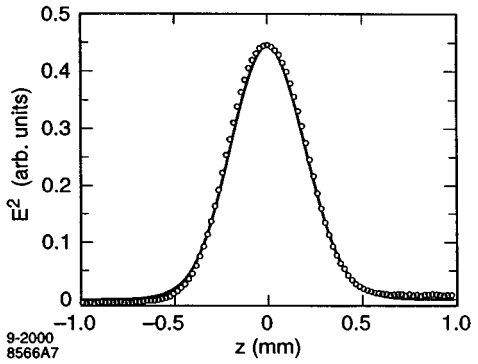

Fig. 5. Result for inferred axial electric field E_z from bead–pull measurement, overlaid with theory. The z-coordinate is as shown in Fig. 2, with the bead pull along the beam axis.

in the course of chemical cleaning. A bead pull was also performed, with the measurement seen in Fig. 5, overlaid with the result computed with the frequency-domain module of *GdfidL*. The dielectric bead was formed by tieing a knot in a length of surgical fiber made of nylon.

The field profile data seen in Fig. 5 permit one to go on to infer peak electric field from cavity voltage, with the result $V_c/E_{\rm pk} \approx 6.14 \times 10^{-4}$ m. Using (4), one may then infer a peak field from the power radiated. With $[R/Q] \approx 110\,\Omega$ from numerical simulation (*GdfidL*), and $Q_e \approx 571$ from measurement, a figure of $P_{\rm out} \approx 1$ kW corresponds to a cavity voltage of 7.9 kV, and a peak field of $E_{\rm pk} \approx 12.9$ MV/m.

V. Conclusions

The bench measurements and simulations presented in this paper indicate that fabrication of and bench measurement on a high-Q millimeter-wave waveguide-coupled resonator are, in practice, quite feasible. Results presented here provide the basis for understanding of the cavity interaction with a beam. This cavity has subsequently been installed on a 300-MeV 0.5-A beam line at the Stanford Linear Accelerator Center (SLAC), Stanford, CA, producing peak power in the range of 1 kW, which will be the subject of a future paper.

Acknowledgment

The authors thank G. Caryotakis, Stanford Linear Accelerator Center (SLAC), Stanford University, Stanford, CA, J. Huth, Harvard University, Cambridge, MA, O. Millican, SLAC, Stanford University, Stanford, CA, D. Shelly, SLAC, Stanford University, Stanford, CA, and A. Farvid, SLAC, Stanford University, Stanford, CA, for their assistance.

References

[1] D. H. Whittum, "Ultimate gradient in solid-state accelerators," in *Proc. Adv. Accelerator Concepts Workshop*.
[2] G. Caryotakis, "High power microwave tubes: In the laboratory and on-line," *IEEE Trans. Plasma Sci.*, vol. 22, pp. 683–691, Oct. 1994.
[3] ——, "The Klystron: A microwave source of surprising range and endurance," *Phys. Plasmas*, vol. 5, pp. 1590–1598, 1998.
[4] D. H. Whittum, "Introduction to Microwave Linacs," in *Techniques and Concepts of High-Energy Physics*, T. Ferbel, Ed. Norwell, MA: Kluwer, 1999, vol. X, pp. 387–486.
[5] W. Bruns, "GdfidL: A finite difference program for arbitrarily small perturbations in rectangular geometries," *IEEE Trans. Magn.*, vol. 32, pp. 1453–1456, May 1996.
[6] *High Frequency Structure Simulator*, Ansoft Corporation, Pittsburgh, PA.
[7] N. M. Kroll and X. E. Lin, "Computer Determinations of the Properties of Waveguide Loaded Cavities," in *Proc. Linear Accelerator Conf.*, C. Beckmann, Ed., Abuquerque, NM, 1990, pp. 238–240.

Design of a Low-Cost 2-D Beam-Steering Antenna Using Ferroelectric Material and the CTS Technology

Magdy F. Iskander, Zhengqing Yun, Zhijun Zhang, R. Jensen, and S. Redd

***Abstract*—The design of a new low-cost antenna array with two-dimensional beam-scanning capability is presented in this paper. The design procedure is based on the continuous transverse stub (CTS) technology and the use of ferroelectric material. With the application of a low-loss ferroelectric material barium strontium titanium oxide with 40% oxide III, beam-scan capability from −60° to 60° was achieved. The tradeoffs in selecting the ferroelectric material and between losses and bias voltage in the CTS design were also examined. Furthermore, it was found necessary to adjust the dimensions of the radiating stubs, as well as the connecting sections of the feed waveguide so as to eliminate reflections between the stubs and, hence, maintain the desirable radiation pattern. It is shown that the use of an average height for the feed waveguide will result in deterioration in the radiation pattern.**

***Index Terms*—CTS, ferroelectric material, low cost, phased array, 2-D beam steering.**

I. Introduction

The design of a low-cost antenna array with two-dimensional (2-D) steering capability is critically important for the commercial success of the satellite industry in broad consumer markets. As the satellite and mobile wireless communications technologies continue to utilize higher frequencies in the 20–60-GHz range, the design

Manuscript received February 1, 2000; revised November 30, 2000.
The authors are with the Electrical Engineering Department, University of Utah, Salt Lake City, UT 84112 USA.
Publisher Item Identifier S 0018-9480(01)03305-1.

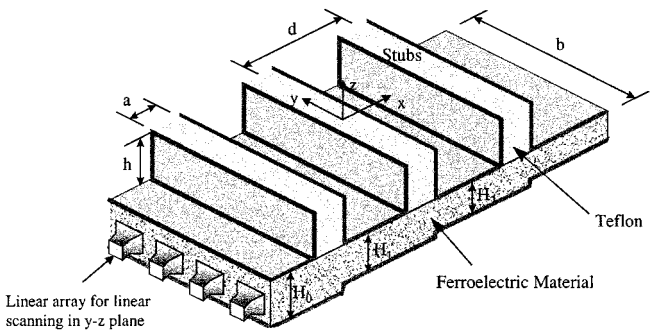

Fig. 1. CTS design with ferroelectric material fill for beam scanning in the $x-z$-plane. Beam scanning in the $x-y$-plane may be achieved either mechanically or using a linear array. For the ferroelectric filled array design, the waveguide width $b = 7.62$ cm, while variable heights of main waveguide were used to eliminate reflections between successive stubs.

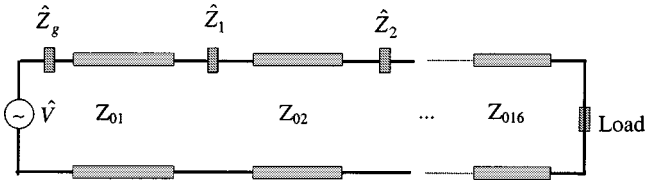

Fig. 2. Transmission-line representation of CTS structure. $\hat{V}$ and $\hat{Z}_g$ are source parameters, $\hat{Z}_1, \hat{Z}_2, \ldots, \hat{Z}_{15}$ are the input impedance of the stubs, and $Z_{01}, Z_{02}, \ldots, Z_{016}$ are the characteristic impedance of the feed waveguide sections of the parallel-plate waveguides.

of a phased-array antenna becomes prohibitively expensive and the realization of 2-D scanning capability to track the satellite or to provide adequate urban wireless communications systems becomes increasingly difficult to realize at a sufficiently low cost suitable for the consumer market. In this paper, we describe the design of a new low-cost antenna array with 2-D scanning capability. The design approach utilizes the continuous transverse stub (CTS) technology invented by Hughes [1], [2] and extends the design procedure to include the use of a suitable ferroelectric material to achieve the 2-D scan. Based on careful examination of the loss tangent, tunability, and the required biasing characteristics of several new barium strontium titanium oxide (BSTO) ferroelectric materials, it is shown that it is possible to achieve a successful design in the 20–60-GHz frequency range. In this case, one-dimensional beam steering will be achieved using a linear phased array as feed or using a sectoral horn feed and mechanical steering, while the steering in the second direction will be achieved through the biasing of the ferroelectric material [3]. In a circular arrangement of the array, it is possible to achieve the 2-D steering using multiplexing together with the ferroelectric material [4].

II. Selection of Ferroelectric Materials

To achieve 2-D scanning, ferroelectric materials are used to fill the main parallel-plate waveguide, as shown in Fig. 1. There are three important parameters to keep in mind while choosing the proper ferroelectric material. This includes the loss tangent, tunability, and required bias voltage to obtain maximum tunability.

Low-loss tangent means less attenuation due to dielectric losses and allows for the use of more array elements to increase the ability to shape the beam. Loss tangents of various compositions of BSTO were examined and, based on available data from the Army Research Laboratory, Aberdeen Proving Grounds, MD [5], it was decided to use $Ba_{60}Sr_{40}TiO_3$, which has dielectric-constant values of unbiased 416.4, biased 333.91, and a loss tangent of 0.0009. The tunability of a material, on the other hand, is defined as

$$\text{Tunability} = \frac{\varepsilon_1 - \varepsilon_2}{\varepsilon_1}$$

where ε_1 is the unbiased dielectric constant and ε_2 is the biased one. A large value of tunability is favorable to achieve a large scanning angle. The tunability of the selected ferroelectric material is 19.81%. The thickness of the ferroelectric material and the required bias voltage are also important parameters. This is because a ferroelectric material typically requires 0.7~3.0 V/μm to sufficiently change the permittivity to obtain maximum tunability. The tradeoff between maintaining a sufficiently small thickness to reduce the bias voltage and the subsequent reduction in the impedance of the feed parallel-plate waveguide should also be considered. A reduction in the waveguide impedance results in large currents and, hence, an increase in the ohmic losses.

III. Design Procedure

Besides the selection of a suitable ferroelectric material, the design procedure included the following steps.

- Step 1) Calculation of the input impedance of the radiating stubs using a finite-difference time-domain (FDTD) code. These calculations included mutual coupling effects [3].
- Step 2) Representation of the CTS structure with tandem sections of transmission lines. The stub discontinuity impedance, including radiation impedance, was placed between these sections, as shown in Fig. 2.
- Step 3) Use of a cascaded transmission-line code to calculate the input impedance and, hence, achieve acceptable broad-band impedance-matching characteristics for the ferroelectric material loaded CTS array. Calculations were made based on the average dielectric values between the biased and unbiased cases.
- Step 4) From the T-line program [6], the voltage across each radiating stub (represented by a lumped impedance element) was calculated (magnitude and phase), and these values were used to calculate the radiation characteristics of the array. It was necessary to change the waveguide height or width in different sections of the transmission line to minimize impedance mismatch and also to maintain the desired phase relationship ($\lambda/2$) between the radiating elements.
- Step 5) A phased-array program was then used to calculate the resulting radiation pattern. These calculations were based on the magnitude and phase of the voltage distribution across the radiating elements.

IV. Results

Selected ferroelectric material is $Ba_{60}Sr_{40}TiO_3$ (40% Oxide III) with dielectric constant of 416.4, loss tangent of 0.0009, and tunability of 19.81. A CTS with 15 radiating stubs was simulated at a frequency of 20 GHz. The height of the main waveguide was made variable to achieve a continuous impedance matching along the CTS structure, as shown in Fig. 1. The values of the waveguide heights $H_0 \sim H_{15}$ and the impedance for each waveguide section are listed in Table I.

It should be noted that it is possible to maintain the same feed waveguide height throughout the CTS structure and adjust the width of the top conductor to account for the desired distribution of the impedance values.

TABLE I
HEIGHT AND IMPEDANCE FOR SECTIONS OF THE MAIN WAVEGUIDE

Section #	0	1	2	3	4	5
Height (cm)	2.65	2.54	2.44	2.33	2.22	2.11
Impedance: unbiased (ohm)	6.43+j0.08	6.12+j0.08	5.90+j0.07	5.64+j0.07	5.37+j0.06	5.11+0.05
Impedance: biased (ohm)	7.03-j0.0032	6.74-j0.0030	6.45-j0.0029	6.16-j0.0028	5.88-j0.0026	5.59-j0.0025

Section #	6	7	8	9	10
Height (cm)	2.00	1.89	1.78	1.67	1.56
Impedance: unbiased (ohm)	4.85+j0.05	4.58+j0.04	4.32+j0.04	4.05+j0.03	3.79+0.03
Impedance: biased (ohm)	5.30-j0.0024	5.01-j0.0023	4.72-j0.0021	4.43-j0.002	4.14-j0.0019

Section #	11	12	13	14	15
Height (cm)	1.46	1.35	1.24	1.13	1.02
Impedance: unbiased (ohm)	3.53+0.02	3.26+j0.02	2.99+j0.01	2.73+0.005	2.47-0.001
Impedance: biased (ohm)	3.86-j0.0017	3.57-j0.0016	3.28-j0.0015	2.99-j0.0013	2.70-j0.0012

The stub widths (a) were assumed uniform and equal to 1.38 mm and the stub heights (h) were also assumed uniform and equal to 0.09833 mm. This results in a constant stub input impedance $Z_1 = Z_2, \ldots = Z_{15} = 0.2639 + j0.0056\ \Omega$. The electric distance between stubs (d) in air is 0.46 of the wavelength in air. The calculated input impedance of each stub was $0.5573 - j1.259$. It should be noted that unlike the present design, earlier CTS design [1] did not encounter the variable impedance sections feature; this is because no steering capability in the x–z-direction was required and the electrical distance between the stubs was maintained at approximately 0.5λ. Therefore, the electric distance between stubs and the impedance of the feed waveguide remained constant throughout the CTS array. For ferroelectric filled feed waveguide, however, the dielectric properties change with the bias voltage and, hence, both the electric distance and characteristic impedance change with the value of the applied bias voltage. These changes cause reflections along the feed waveguide and, hence, result in arbitrary voltage distributions (magnitude and phase) across the stubs. This, in turn, causes deterioration in the resulting radiation pattern. Variation in the height of the feed waveguide sections and also of the height of the stubs were used to achieve impedance matching (real and imaginary parts) along the feed waveguide and, hence, maintain in-phase voltage distributions at the various stubs. The resulting design is shown in Fig. 1.

Fig. 3 shows the radiation pattern of a CTS with BSTO filler with and without bias. It can be seen that a scanning range from -60° to 60° can be achieved by biasing the selected ferroelectric material with tunability of 19.81%.

It is interesting to examine the radiation characteristics and the possible deterioration in the radiation pattern when a constant value of the waveguide height is used in the design. Fig. 4 shows the resulting radiation pattern for the cases of unbiased ferroelectric (beam is at -60°), half biased (beam is at 0°) and the full biased case (beam at 60°) for three cases of the waveguide height. This includes $H = 1.01$ cm (corresponding to the smallest height in the implemented design), $H = 2.65$ cm (largest height), and $H = 1.83$ cm, which corresponds to the average of the various heights implemented in the simulated design. As it may be seen, basing the design on the largest value of H results in a least distorted beamwidth value. Besides an increase in the sidelobe values, the beamwidth was also broadened. It may also be worth noting that the implemented design was based on the fact that the electric distance between the stubs is 0.5λ at half bias and, hence, the no change condition shown in Fig. 4(b).

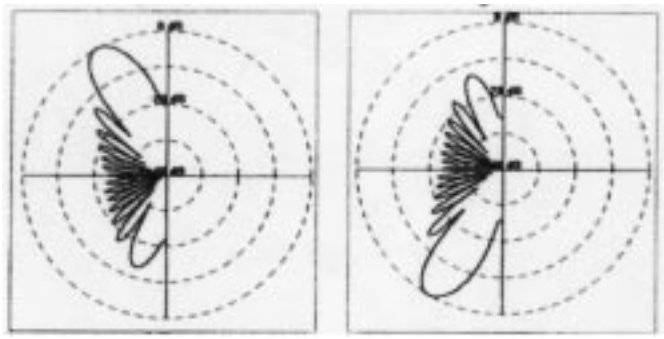

(a) (b)

Fig. 3. Radiation patterns of the designed 15-element CTS array. (a) Scanning angle $= -60^\circ$. (b) Scanning angle $= 60^\circ$.

Fig. 5 shows a comparison of the radiation patterns for the case when H was taken as the largest height of the feed waveguide ($H = 2.65$ cm). As it may be noted, degradation in the radiation pattern includes broader beamwidth and increase in the sidelobe level. It is undesirable to continue to increase the height of the feed waveguide because this will result in an increase in the required value of the bias voltage. Therefore, this tradeoff needs to be seriously considered in designing the ferroelectric-based CTS antennas.

V. DISCUSSIONS

With the exciting result of possibly steering the radiation beam from -60° to 60° by biasing the ferroelectric material, more careful design considerations such as attenuation and conduction losses need to be considered. Based on conduction loss calculations using a microstrip-line type of arrangement, it may be shown that conductor losses are high, particularly as the height of the parallel-plate waveguide is decreased to reduce the required biasing voltage [3]. For

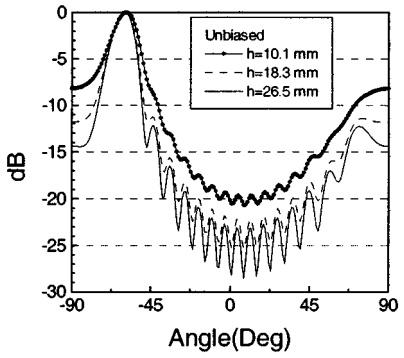

(a)

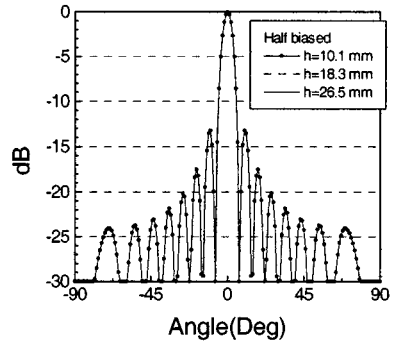

(b)

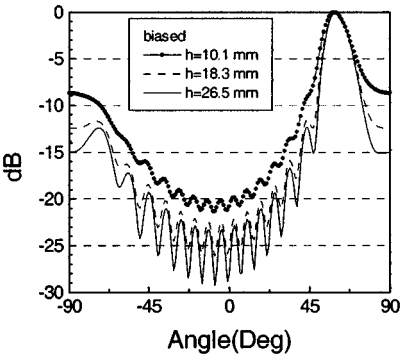

(c)

Fig. 4. Radiation patterns for three different biases voltages and three constant heights of the feed waveguide. Improved performance may be achieved when a larger constant heights were selected. (a) Unbiased. (b) Half biased. (c) Full biased.

example, for $f = 30$ GHz and the thickness of the conductor equal to 0.1 mm, the conductor loss of the selected BSTO material is 23.35 dB (unbiased) and 21.44 dB (biased) when the height of the parallel-plate waveguide (H) is 0.10 mm. This high value can be overcome by increasing the height of the waveguide and, hence, increasing the waveguide impedance. For example, for a waveguide height of 0.3 mm, the conductor loss was reduced to 7.45 dB (unbiased) and 6.85 dB (biased), but this will be achieved at the expense of a much higher biasing voltage and the potential for dielectric breakdown, particularly at interface.

To overcome these conductor losses, we are currently evaluating an optimization process whereby a multilayer structure will be used. In a parallel-plate waveguide and if a multilayer dielectric including ferroelectric ones were used, it is possible to excite longitudinal section electric (LSE) and longitudinal section magnetic (LSM) waves, which helps confine the fields at the interface between the ferroelectric and low dielectric-constant materials placed at the center of the waveguide.

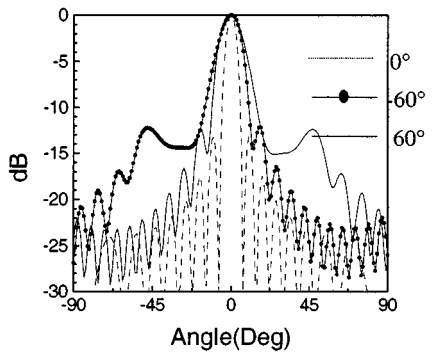

Fig. 5. Radiation patterns for feed waveguide with uniform height $H = 2.65$ cm. Results from three beam angles at -60°, 0°, and 60° are overlapped to graphically illustrate and compare the resulting deterioration in the radiation pattern. Note that, for the purpose of comparison, all three patterns are plotted with a main beam in the same directions.

Initial results from this effort are encouraging, and a detailed description of this study will be reported in a future paper.

REFERENCES

[1] W. W. Milroy, "Continuous transverse stub element devices for flat plate antenna arrays," U.S. Patent 5 483 248, Jan. 9, 1996.

[2] A. Lemons, R. Lewis, W. Milroy, R. Robertson, S. Coppedge, and T. Kastle, "W-band CTS planar array," in *IEEE MTT-S Int. Microwave Symp. Dig.*, vol. 2, 1999, pp. 651–654.

[3] M. F. Iskander, Z. Yun, R. Jensen, and S. Redd, "Design of low cost 2D beam steering antenna using the CTS technology," in *USNC/URSI Radio Sci. Meeting Dig.*, July 1999, p. 240.

[4] Z. Zhang, M. F. Iskander, and Z. Yun, "Coaxial continuous transverse stub element device antenna array," U.S. Patent 6 201 509, Mar. 13, 2001.

[5] Microwave ferroelectrics (1997). [Online]. Available: http://horse.arl.mil:80/FERRO/

[6] M. F. Iskander and E. Jensen, "TLine: Software for sinusoidal steady-state analysis of transmission lines," *Comput. Applicat. Eng. Educ.*, vol. 2, no. 3, pp. 185–194, 1994.